Density Functional Study of Methyl Radical Association Kinetics

Jingjing Zheng, Shuxia Zhang, and Donald G. Truhlar*

Department of Chemistry and Supercomputing Institute, University of Minnesota, 207 Pleasant Street S.E., Minneapolis, Minnesota 55455-0431

Rate constants of the prototypical methyl−methyl radical association reaction are calculated on the basis of variational transition-state theory with a variable reaction coordinate and a multifaceted dividing surface. The potential energies required in the Monte Carlo integrations are evaluated directly using the M06 and M06-L density functionals. The rate constants are calculated at the canonical, microcanonical, and *E,J*-resolved microcanonical levels. The best prediction of rate constants is based on the potential energies calculated by the M06-L density functional; these agree with experimental data quantitatively from 300 to 1000 K. This study shows that density functional theory can be accurate enough for calculating rate constants of reactions with loose transition states, whereas previously only multireference wave function methods, which are more complicated and more expensive, had been demonstrated to be sufficiently accurate. The application of density functional theory for the loose transition states will allow larger and complicated systems to be studied efficiently.

1. Introduction

The quantitative prediction of accurate rate constants for barrierless radical−radical association reactions involves two challenges:[1−3] (i) the use of flexible enough dividing surfaces to define the variational transition state; (ii) the use of accurate enough potential energy surfaces calculated by electronic structure theory. In the transition-state region of a barrierless reaction, a number of rotational modes transform from free rotations to hindered rotations and eventually to rigid bending vibrations. This process is typically associated with large vibrational anharmonicity and vibrational Coriolis coupling. The decoupled rigid-rotor harmonic-oscillator treatment, which is often a good approximation for tight transition states, is not accurate for the anharmonicity and the coupling between the various modes for the loose transition state in a barrierless association reaction.[1] Potential energy surfaces for this kind of reaction are usually required to be accurate for the region in which the forming bond distance is 1.5−6.0 Å and for all orientations of the two fragments. A difficulty with calculating potential energy surfaces in this region, especially the region in which the forming bond distance is greater than 2 Å, is the multireference character[4] of the electronic wave function for systems with partially broken bonds. Thus one must use electronic structure methods suitable for multireference systems. Unlike single-reference electronic structure methods, multireference wave function methods are not black-box methods, and the best choice of reference state is system dependent. Multireference wave function methods that include dynamical correlation energy are also generally very computationally expensive.

A variable reaction coordinate formulation of variational transition-state theory (VTST) has been shown to provide useful accuracy for many barrierless association reactions.[2,3,5−7] In this approach, the dividing surfaces are defined in terms of pivot points tied to each of the reacting fragments. Variable choices of the number and location of these pivot points yield different definitions of the reaction coordinates and hence of the generalized transition-state theory dividing surface (which is called a generalized transition state), and the reactive flux is variationally minimized both with respect to these choices and with respect to the distance between pivot points in the two reactants. Georgievskii and Klippenstein provided an efficient way to implement this in VTST.[8,9] This involves Monte Carlo integration of the coordinate space degrees of freedom of the classical phase space representation of the generalized transition-state partition function for arbitrary orientations of the reactants over a wide range of interfragment separations. In the critical range of distance, the valence interactions and the long-range van der Waals interactions are of comparable magnitude. Transition states of radical−radical associations usually have multireference character due to electronic near degeneracy, which leads to geometry-dependent nondynamical correlation effects. In these cases, single-reference electronic wave function methods and popular density functionals can fail dramatically. Therefore, multireference wave function methods, especially complete-active-space second order perturbation method (CASPT2)[10,11] and multireference configuration interaction (MR-CI) theory,[12,13] are extensively used to calculate potential energy surfaces for radical−radical association reactions.[14,15] A multiconfigurational complete active space self-consistent-field (CASSCF) calculation is used to generate orbitals for such multireference calculations, and a good starting guess for the electronic wave function is essential for correct convergence of the CASSCF iterations. Adequate guesses are usually geometry dependent. However, in doing a direct dynamics calculation using Monte Carlo integration, geometries are chosen randomly, and this problem can lead some calculations to fail

---

* Corresponding author. E-mail: truhlar@umn.edu.

to converge or to converge incorrectly. To avoid these errors, one has to monitor every point in the calculation and redo some suspicious points using a different starting guess, which is inefficient.[16]

The development in recent years[17,18] of improved density functionals provides us with an alternative way to evaluate potential energy surfaces in the region where valence and noncovalent interactions are both important. Two new functionals, M06-L and M06, provide improved ability to simultaneously describe both multireference systems and transition states, and in addition they are both much more accurate than popular density functionals for noncovalent interactions.[17,18] M06-L is a local density functional, which is expected to be most suitable for describing systems with multireference character, whereas M06 has better performance for barrier heights, which may be a less important consideration for barrierless reactions. Because density functional theory is formally a single-configuration method, it avoids the problem of obtaining starting guess orbitals for multiconfigurational reference states at each geometry. Density functional theory is also much more affordable than multireference methods.

The importance of the prototypical methyl−methyl radical association reaction in combustion chemistry is a primary motivation for numerous investigations of its rate, by both experiment[19−28] and theory.[14,16,22,28−51] Because a large number of experimental measurements are available, this reaction also has been a workhorse to examine the quantitative accuracy of theoretical methods to predict radical−radical barrierless association reactions. Klippenstein and co-workers have computed quantitatively accurate association rate constants of this reaction for temperatures below 500 K using variable-reaction-coordinate transition-state theory.[14] They employed direct evaluation of the orientation-dependent potential energies at the CASPT2/cc-pVDZ level. The resulting potential energy surface was then corrected using one-dimensional orientation-independent energy corrections obtained from CAS+1+2+QC/aug-cc-pVTZ calculations along the $CH_3 + CH_3$ minimum energy path (MEP), where CAS+1+2 denotes MR-CI with single and double excitations from a CASSCF reference, and +QC denotes a Davidson correction for higher excitations. The reason for employing the lower-level CASPT2/cc-pVDZ calculation for the energy along the reaction path is that CAS+1+2+QC is not size-consistent, but CASPT2 has no such problem; furthermore, the use of the lower level with a double-ζ basis set makes the computational cost of direct dynamics more feasible. However, the CASPT2/cc-pVDZ method significantly underestimates the interaction energies of two methyl radicals.[14] The authors chose CAS+1+2+QC/aug-cc-pVTZ calculations to make corrections because the CAS+1+2+QC approach treats dynamical correlation energy more completely, and some sample calculations suggested that away from the minimum energy path the CAS+1+2+QC approach may be more accurate than CASPT2.[14] The calculations in ref 14 assume that the higher-level correction is independent of orientation, but this assumption has not been validated due to the multidimensional nature of the $CH_3 + CH_3$ reaction.

In the present work, we will adopt M06-L/MG3S and M06/MG3S for the direct dynamics without any orientation-independent correction at another theory level. Note that the MG3S basis set[52−57] is equivalent to 6-311+G(2df,2p)[52−54] for C and H. We find that the SCF iterations converge well for these calculations so we avoid the problem of a good starting guess for multiconfigurational reference states. The computational efficiency of DFT makes it possible to directly evaluate

the potential energy surface with the augmented and multiply polarized triple-ζ MG3S basis set.

2. Methodology

The kinetics calculations are based on variational transition-state theory with a variable reaction coordinate and a multifaceted dividing surface. The details of this theory can be found in the work of Georgievskii and Klippenstein.[8,9] Therefore, only a brief review relevant to the present work is provided here.

The use of the variable reaction coordinate formalism assumes that the contribution of the vibrational modes of the reactants, called "conserved modes," to the transition-state partition function is canceled by the corresponding contribution to the reactant partition function. It also assumes that the internal geometries of reactants do not change along reaction path. The reaction coordinate s is defined by the distance between a pivot point on one reactant and that on another.[8] According to the variational principle of TST,[58] the locations of the pivot points and the distances between them are optimized to minimize the reaction rate. For methyl radical association, there are two sites for each methyl radical, one on each side of the CH_3 plane along the C_3 axis. In sampling over orientations, the directions of three three vectors are sampled over the whole phase space. One is the vector connecting pivot points on different reactants, and the other two are vectors connecting the center of mass of a methyl group to one of the pivot points of that methyl group. The lengths of these vectors are fixed during the sampling over their orientations. A four-faceted dividing surface is formed by the four pivot points. In this work, the pivot points are fixed at the optimal value[14] of 0.25 Å along the C_3 axis. The distances between the pivot points on different methyls are varied from 1.7 to 7.0 Å with a 0.1 Å grid size. Note that we used the full multifaceted method of ref 9, not the infinite boundary approximation used in ref 14.

The high-pressure limit rate constant at the temperature T can be expressed as[9,33,59]

$$k(T,s) = \frac{\hbar^2}{2\pi} g_e \frac{\sigma_1 \sigma_2}{\sigma^\ddagger Q_1 Q_2} \left(\frac{2\pi}{\mu k_B T}\right)^{3/2} \int dE \, e^{-E/k_b T} \, dJ \, N(E,J,s)$$

(1)

where s is the value of reaction coordinate, which is defined above as the distance between two pivot points; g_e is the ratio of the electronic partition function of the transition state to the product of the electronic partition functions of reactants; μ is the reduced mass; Q_1 and Q_2 are the rotational partition functions of the reactants calculated without symmetry numbers; J is the unitless total angular momentum quantum number; $N(E,J,s)$ is the number of accessible states of the generalized transition state s for total energy E and angular momentum $J\hbar$; and σ_1, σ_2, and $\sigma^\ddagger$ are the rotational symmetry numbers for the reactants and transition state, respectively. Because methyl radical has D_{3h} symmetry, its rotational symmetry number is 6.[60] The effective rotational symmetry number of the transition state is 72. We set g_e equal to 0.25.

We consider three ways to perform variational calculations, which correspond to optimizing the transition-state dividing surface for three different ensembles: (i) for canonical variational theory (CVT), $N(E,J)$ is calculated for all E and J at a single s value. Then the rate constant $k(T,s)$ is minimized with respect to s for each T. (ii) For microcanonical variational theory (μVT), in eq 1 the integral over J is carried out first with E fixed to get $N(E)$. Then $N(E)$ is minimized with respect to s for each E, and the optimized $N(E)$ is used for the integral over E. (iii) For

Letters

J. Phys. Chem. A, Vol. 112, No. 46, 2008 **11511**

energy and total angular momentum resolved microcanonical variational theory (E,J-μVT), $N(E,J)$ is minimized with respect to s for each E and J. Then the integral is calculated using the optimized $N(E,J)$.

In our work the integrals over E and J in eq 1 are approximated by 4-point Gauss−Laguerre and 61-point Simpson's rule quadratures, respectively. Convergence was checked by higher-order Gauss−Laguerre quadrature for the integration over E. The angular momentum quantum number J covers the range from 0 to 300 with step size 5.

In principle, the rate constants should be corrected to take account of geometry relaxation of the reactants along the MEP; e.g., in previous work, this correction was estimated without any dependence on their orientations. This geometry relaxation effect is not taken into account in the present study for three reasons: (i) a one-dimensional geometry relaxation correction may not apply to all the orientations as assumed previously to make the calculation practical;[14] (ii) a geometry relaxation correction conflicts with the assumption of that the partition functions of conserved modes cancel between reactant and generalized transition states, and (iii) sample calculations reported by Klippenstein et al.[14] indicate that assuming cancelation of the reactant and transition-state partition function for conserved modes is good to 20% or better for the present reaction up to 2000 K. Klippenstein et al. nevertheless included such a correction plus an estimated recrossing factor of 0.85 obtained from direct B3LYP/6-31G* trajectory simulations,[14] but the calculations reported here do not include such corrections. Note that a recrossing calculation based on trajectories may overestimate the amount of recrossing due to the non-maintenance of quantum mechanical zero point effects in classical mechanics.

Variable-reaction coordinate VTST has been implemented into a new version of the *POLYRATE* program.[61] The Monte Carlo integration of the classical phase space representation of the transition-state partition function has been massively parallelized in our implementation; the parallel implementation based on Message-Passing Interface (MPI) allows Monte Carlo sampling using hundreds of CPUs very efficiently; 320 cores on 80 processors were used in the present study. *GAUSSRATE*[62] interfaces the *Gaussian 03* electronic structure package[63] and *MN-GFM* module[64] with this new version of the *POLYRATE* program to do the direct dynamics.

The interaction energies required in Monte Carlo integration over all possible orientations of two fragments are calculated "on the fly" using M06 and M06-L density functionals. The computational efficiency of density functional theory allows us to employ an augmented, multiply polarized triple-ζ basis set, namely 6-311+G(2df,2p), in direct dynamical calculations. For each of the four facets of the multifaceted dividing surface, 640 configurations are sampled, for a total sample size of 2560 samples at each s value; this leads to the Monte Carlo errors lower than 10%. We considered 54 s values; thus 138240 interaction energies are calculated in a variational calculation. The SPRNG random number generator (version 2.0)[65] is employed for the parallel Monte Carlo integration; in particular, the modified Lagged Fibonacci Generator (MLFG) in SPRNG package is used. The wall clock time for a variational rate calculation is about 3.5 min per thousand samples when using 40 SGI Altix XE 1300 computer nodes, each containing two quad-core 2.66 GHz Intel Xeon "Clovertown"-class processors sharing 16 GB of main memory−320 cores in total.
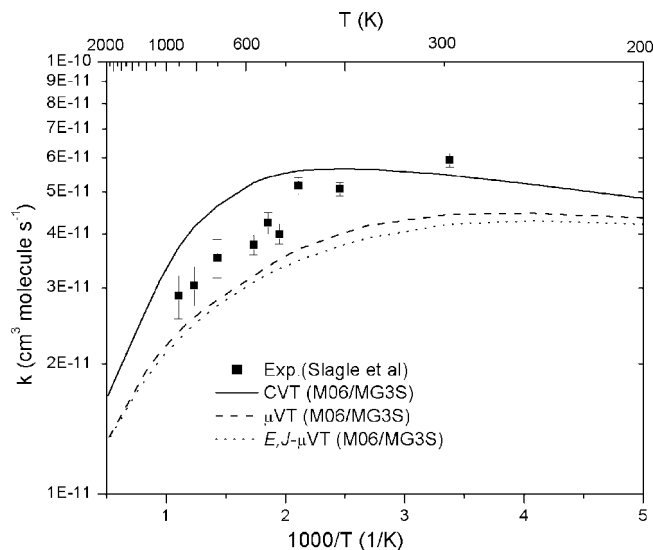
Figure 1. Calculated rate constants using the M06/MG3S potential energy surface compared to experimental data.
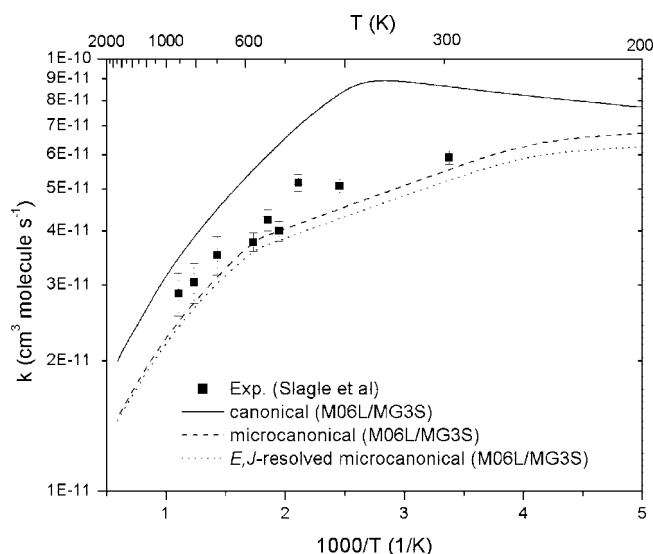
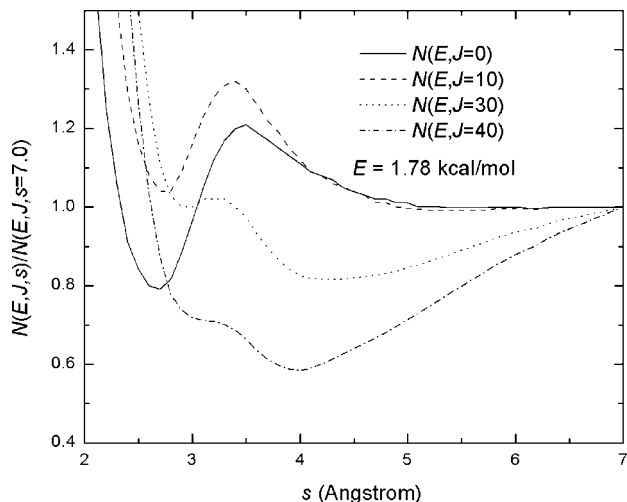

Figure 2. Calculated rate constants using the M06-L/MG3S potential energy surface compared to experimental data.

## 3. Results and Discussion

The calculated rate constants for the M06 and the M06-L density functionals are plotted in Figures 1 and 2 together with the high-pressure experimental data from Slagle et al.[21] The μVT and E,J-μVT rate constants are very similar with 10% or less difference in both the M06 and M06-L cases. This difference is comparable with the Monte Carlo uncertainties. However, CVT rate constants are much higher than μVT and E,J-μVT ones with differences larger than 20% or even much more. The difference is explained by the fact that the values of s that minimize $N(E)$ or $N(E,J)$ vary over a wide range. Figure 3 shows the dependence of $N(E,J,s)$ on s for a range of J values at $E =$ 1.78 kcal/mol, where the zero of energy corresponds to two infinitely separated methyl radicals at rest at their classical equilibrium geometries. Especially when the separation of two methyl radicals is larger than 2.5 Å, where the minima of $N(E,J)$ are located, the changes of $N(E,J,s)$ are slow compared to the values at smaller s values. This behavior explains why the μVT and E,J-μVT rate constants are very close.

Figure 3 also demonstrates some common characteristics of loose transition states. For a small J value ($J = 0$ or 10), $N(E,J)$

Figure 3. The *E,J*-resolved number of states, *N(E,J)*, normalized to its value at large separation of the pivot points, $s = 7.0$ Å. The total energy *E* is 1.78 kcal/mol. Data are from M06-L calculations.
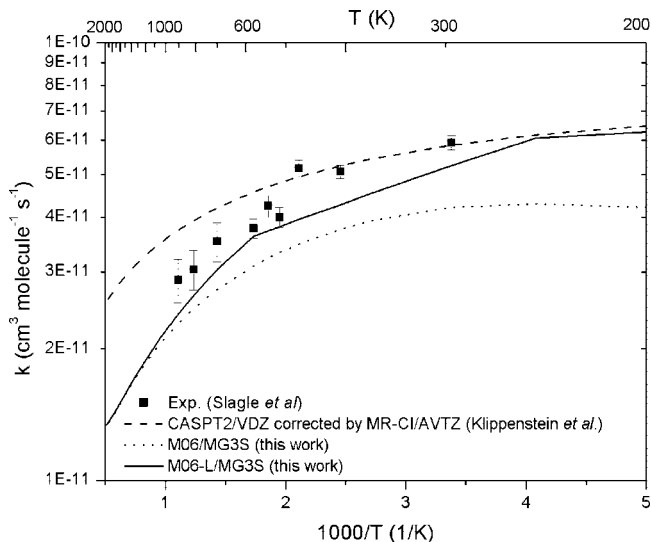
Figure 4. *E,J-μ*VT rate constants using various potential energy surfaces compared to experimental data.

reaches a minimum, called the inner minimum, at a relatively small *s* value around 2.6 Å. Its location is determined by the balance of entropy and enthalpy effects. As *J* increases, another minimum, called outer minimum appears and moves toward smaller *s*. The outer minima are located at quite large separations and are dominated by centrifugal effects. The centrifugal barrier becomes the dominant factor for large *J* values, e.g., *J* = 40, and it tends to make the inner minimum disappear.

The *E,J-μ*VT M06/MG3S and M06-L/MG3S rate constants agree with the experimental data quite well as shown in Figures 1, 2, and 4. For tight transition states, the hybrid meta GGA functional M06 has been found to be[18] more accurate than local meta functional M06-L.[17,66] However, rate constants using the M06-L functional agree better with experimental values than those obtained with the M06 functional. This is due to the multireference character of loose transition states of radical association reactions.

Figure 4 also compares the present *E,J-μ*VT results with the theoretical rate constants of Klippenstein et al.[14] In the Klippenstein et al. work,[14] the potential energies were calculated using the CASPT2/cc-pVDZ method during Monte Carlo sampling. Then, because the CASPT2/cc-pVDZ potential sig-

nificantly underestimated the reaction rates, these orientation-dependent potential energies were corrected by the one-dimensional energy along the minimum energy path calculated at the theory level of CAS+1+2+QC/aug-cc-pVTZ. As discussed in the Introduction, this one-dimensional correction has never been validated. For this reason and because Klippenstein et al. also employed a geometry relaxation correction, it is impossible to provide a succinct summary of the reasons why the two sets of calculations differ.

The M06-L results are quite close to those calculated by multireference methods at low temperatures, where variational transition states are located at large separations of reactants. In fact, the differences are close to Monte Carlo integration uncertainities at temperatures below 500 K. The difference between M06-L and multirefence methods is larger for higher temperature. The M06-L results agree better with experimental data for temperatures higher than 500 K although these experimental data are believed not to have fully reached the high-pressure limit. Because the most important variational transition states at high temperature are located at short distances ($s = 2.0-3.0$ Å), the most important part of the potential energy surface is more anisotropic than at high temperature. The one-dimensional orientation-independent correction of previous work is therefore questionable, whereas our M06 and M06-L calculations sample potential energy directly without any corrections.

The predicted reaction rates using the M06-L potential energy surface agree with experimental data not only at low temperature but also at high temperature. The high-pressure limit rate constants calculated by using the M06-L potential energy surface are well reproduced by the following modified Arrhenius expression (*k* in cm³ molecule⁻¹ s⁻¹ and *T* in K):

$$k(T) = 9.78 \times 10^{-9} T^{-0.863} \exp(-97.75/T) \qquad (2)$$

4. Conclusions

"The difficulty in efficiently generating accurate estimates for the radical-radical interaction energies has greatly hindered the application of the VRC-TST approach."[14] (VRC-TST denotes variable-reaction-coordinate transition-state theory.) The present calculations show that the new M06-L density functional is capable of accuracy as good as more expensive and more troublesome high-level wave function calculations for calculating radical association rate constants. Density functional theory is applicable to large, complex systems because the cost scales as N^4 and N^3 for hybrid and local density funcitonals, respectively, whereas including dynamical correlation by wave function methods scales as N^5 for CASPT2 and as N^6 for MR-CI with single and double excitations.

The variable-reaction-coordinate multifaceted-dividing-surface option for variational transition-state theory has now been added to a new parallel version of the freely available *POLYRATE* computer code,[61] which is also interfaced with *Gaussian 03*.[62,63]

References and Notes

(1) Yu, J. W.; Klippenstein, S. J. *J. Phys. Chem.* **1991**, *95*, 9882.
(2) Truhlar, D. G.; Garrett, B. C.; Klippenstein, S. J. *J. Phys. Chem.* **1996**, *100*, 12771.
(3) Fernandez-Ramos, A.; Miller, J. A.; Klippenstein, S. J.; Truhlar, D. G. *Chem. Rev.* **2006**, *106*, 4518.

Letters

J. Phys. Chem. A, Vol. 112, No. 46, 2008 **11513**

(4) Truhlar, D. G. *J. Comput. Chem.* **2007**, *28*, 73.

(5) Klippenstein, S. J. *Chem. Phys. Lett.* **1990**, *170*, 71.

(6) Klippenstein, S. J. *J. Chem. Phys.* **1991**, *94*, 6469.

(7) Klippenstein, S. J. *J. Chem. Phys.* **1992**, *96*, 367.

(8) Georgievskii, Y.; Klippenstein, S. J. *J. Chem. Phys.* **2003**, *118*, 5442.

(9) Georgievskii, Y.; Klippenstein, S. J. *J. Phys. Chem. A* **2003**, *107*, 9776.

(10) Andersson, K.; Malmqvist, P. A.; Roos, B. O.; Sadlej, A. J.; Wolinski, K. *J. Phys. Chem.* **1990**, *94*, 5483.

(11) Andersson, K.; Malmqvist, P. A.; Roos, B. O. *J. Chem. Phys.* **1992**, *96*, 1218.

(12) Brown, F. B.; Shavitt, I.; Shepard, R. *Chem. Phys. Lett.* **1984**, *105*, 363.

(13) Werner, H.-J. *Adv. Chem. Phys.* **1987**, *69*, 1.

(14) Klippenstein, S. J.; Georgievskii, Y.; Harding, L. B. *Phys. Chem. Chem. Phys.* **2006**, *8*, 1133.

(15) Harding, L. B.; Klippenstein, S. J.; Jasper, A. W. *Phys. Chem. Chem. Phys.* **2007**, *9*, 4055.

(16) Klippenstein, S. J.; Harding, L. B. *J. Phys. Chem. A* **1999**, *103*, 9388.

(17) Zhao, Y.; Truhlar, D. G. *Theor. Chem. Acc.* **2008**, *120*, 215.

(18) Zhao, Y.; Truhlar, D. G. *Acc. Chem. Res.* **2008**, *41*, 157.

(19) Glanzer, K.; Quack, M.; Troe, J. *Chem. Phys. Lett.* **1976**, *39*, 304.

(20) Glanzer, K.; Quack, M.; Troe, J. In *Sixteenth Symposium (International) Combustion*; The Combustion Institute: Seattle, WA, 1977, p 949.

(21) Slagle, I. R.; Gutman, D.; Davies, J. W.; Pilling, M. J. *J. Phys. Chem.* **1988**, *92*, 2455.

(22) Walter, D.; Grotheer, H.-H.; Davies, J. W.; Pilling, M. J.; Wagner, A. F. In *Twenty-Third Symposium (International) Combustion*; The Combustion Institute: Seattle, WA, 1990; p 107.

(23) Hwang, S. M.; Wagner, H. G.; Wolff, T. In *Twenty-Third Symposium (International) Combustion*; The Combustion Institute: Seattle, WA, 1990; p 99.

(24) Hwang, S. M.; Rabinowitz, M. J.; Gardiner, W. C. *Chem. Phys. Lett.* **1993**, *205*, 157.

(25) Davidson, D. F.; Dirosa, M. D.; Chang, E. J.; Hanson, R. K.; Bowman, C. T. *Int. J. Chem. Kinet.* **1995**, *27*, 1179.

(26) Du, H.; Hessler, J. P.; Ogren, P. J. *J. Phys. Chem.* **1996**, *100*, 974.

(27) Smith, G. P. *Chem. Phys. Lett.* **2003**, *376*, 381.

(28) Wang, B. S.; Hou, H.; Yoder, L. M.; Muckerman, J. T.; Fockenberg, C. *J. Phys. Chem. A* **2003**, *107*, 11414.

(29) Gorin, E. J. *J. Chem. Phys.* **1939**, *7*, 256.

(30) Quack, M.; Troe, J. *Ber. Bunsen-Ges. Phys. Chem.* **1977**, *81*, 329.

(31) Cobos, C. J.; Troe, J. *J. Chem. Phys.* **1985**, *83*, 1010.

(32) Wardlaw, D. M.; Marcus, R. A. *J. Chem. Phys.* **1985**, *83*, 3462.

(33) Wardlaw, D. M.; Marcus, R. A. *J. Phys. Chem.* **1986**, *90*, 5383.

(34) Evleth, E. M.; Kassab, E. *Chem. Phys. Lett.* **1986**, *131*, 475.

(35) Klippenstein, S. J.; Marcus, R. A. *J. Chem. Phys.* **1987**, *87*, 3410.

(36) Wagner, A. F.; Wardlaw, D. M. *J. Phys. Chem.* **1988**, *92*, 2462.

(37) Smith, S. C.; Gilbert, R. G. *Int. J. Chem. Kinet.* **1988**, *20*, 979.

(38) Darvesh, K. V.; Boyd, R. J.; Pacey, P. D. *J. Phys. Chem.* **1989**, *93*, 4772.

(39) Stewart, P. H.; Larson, C. W.; Golden, D. M. *Combust. Flame* **1989**, *75*, 25.

(40) Aubanel, E. E.; Robertson, S. H.; Wardlaw, D. M. *J. Chem. Soc., Faraday Trans.* **1991**, *87*, 2291.

(41) Forst, W. *J. Phys. Chem.* **1991**, *95*, 3612.

(42) Robertson, S. H.; Wardlaw, D. M.; Hirst, D. M. *J. Chem. Phys.* **1993**, *99*, 7748.

(43) Pitt, I. G.; Gilbert, R. G.; Ryan, K. R. *J. Phys. Chem.* **1995**, *99*, 239.

(44) Robertson, S. H.; Pilling, M. J.; Baulch, D. L.; Green, N. J. B. *J. Phys. Chem.* **1995**, *99*, 13452.

(45) Hessler, J. P. *J. Phys. Chem.* **1996**, *100*, 2141.

(46) Hessler, J. P.; Ogren, P. J. *J. Phys. Chem.* **1996**, *100*, 984.

(47) Jeffrey, S. J.; Gates, K. E.; Smith, S. C. *J. Phys. Chem.* **1996**, *100*, 7090.

(48) Pesa, M.; Pilling, M. J.; Robertson, S. H.; Wardlaw, D. M. *J. Phys. Chem. A* **1998**, *102*, 8526.

(49) Pacey, P. D. *J. Phys. Chem. A* **1998**, *102*, 8541.

(50) Naroznik, M. *J. Chem. Soc., Faraday Trans.* **1998**, *94*, 2531.

(51) Li, H.; Chen, Z.; Huang, M. B. *Int. J. Chem. Kinet.* **2008**, *40*, 161.

(52) Krishnan, R.; Binkley, J. S.; Seeger, R.; Pople, J. A. *J. Chem. Phys.* **1980**, *72*, 650.

(53) Clark, T.; Chandrasekhar, J.; Spitznagel, G. W.; Schleyer, P. V. *J. Comput. Chem.* **1983**, *4*, 294.

(54) Frisch, M. J.; Pople, J. A.; Binkley, J. S. *J. Chem. Phys.* **1984**, *80*, 3265.

(55) Fast, P. L.; Sanchez, M. L.; Truhlar, D. G. *Chem. Phys. Lett.* **1999**, *306*, 407.

(56) Curtiss, L. A.; Redfern, P. C.; Raghavachari, K.; Rassolov, V.; Pople, J. A. *J. Chem. Phys.* **1999**, *110*, 4703.

(57) Lynch, B. J.; Zhao, Y.; Truhlar, D. G. *J. Phys. Chem. A* **2003**, *107*, 1384.

(58) Truhlar, D. G.; Garrett, B. C. *Annu. Rev. Phys. Chem.* **1984**, *35*, 159.

(59) Garrett, B. C.; Truhlar, D. G. *J. Phys. Chem.* **1979**, *83*, 1052.

(60) Fernandez-Ramos, A.; Ellingson, B. A.; Meana-Paneda, R.; Marques, J. M. C.; Truhlar, D. G. *Theor. Chem. Acc.* **2007**, *118*, 813.

(61) Zheng, J.; Zhang, S.; Lynch, B. J.; Corchado, J. C.; Chuang, Y.-Y.; Fast, P. L.; Hu, W.-P.; Liu, Y.-P.; Lynch, G. C.; Nguyen, K. A.; Jackels, C. F.; Ramos, A. F.; Ellingson, B. A.; Melissas, V. S.; Villà, J.; Rossi, I.; Coitino, E. L.; Pu, J.; Albu, T. V.; Steckler, R.; Garrett, B. C.; Isaacson, A. D.; Truhlar, D. G. *POLYRATE*, version 2008; University of Minnesota: Minneapolis, 2008.

(62) Zheng, J.; Zhang, S.; Corchado, J. C.; Chuang, Y.-Y.; Coitiño, E. L.; Ellingson, B. A.; Truhlar, D. G. *GAUSSRATE*, version 2008; University of Minnesota: Minneapolis, 2008.

(63) Frisch, M. J.; Trucks, G. W.; Schlegel, H. B.; Scuseria, G. E.; Robb, M. A.; Cheeseman, J. R.; Zakrzewski, V. G.; Montgomery, J. A.; Stratmann, R. E.; Burant, J. C.; Dapprich, S.; Millam, J. M.; Daniels, A. D.; Kudin, K. N.; Strain, M. C.; Farkas, O.; Tomasi, J.; Barone, V.; Cossi, M.; Cammi, R.; Mennucci, B.; Pomelli, C.; Adamo, C.; Clifford, S.; Ochterski, J.; Petersson, G. A.; Ayala, P. Y.; Cui, Q.; Morokuma, K.; Malick, D. K.; Rabuck, A. D.; Raghavachari, K.; Foresman, J. B.; Cioslowski, J.; Ortiz, J. V.; Baboul, A. G.; Stefanov, B. B.; Liu, G.; Liashenko, A.; Piskorz, P.; Komaromi, I.; Gomperts, R.; Martin, R. L.; Fox, D. J.; Keith, T.; Al-Laham, M. A.; Peng, C. Y.; Nanayakkara, A.; Challacombe, M.; Gill, P. M. W.; Johnson, B. G.; Chen, W.; Wong, M. W.; Andres, J. L.; Gonzalez, C.; Head-Gordon, M.; Replogle, E. S.; Pople, J. A. *Gaussian03*, revision D.01; Gaussian, Inc.: Pittsburgh, PA, 2003.

(64) Zhao, Y.; Truhlar, D. G. *MN-GFM: Minnesota Gaussian Functional Module*, version 3.0; University of Minnesota: Minneapolis, 2007.

(65) Mascagni, M.; Srinivasan, A. Algorithm 806: SPRNG: A Scalable Library for Pseudorandom Number Generation. In *ACM Transactions on Mathematical Software*; 2000; Vol. 26, p 436.

(66) Zheng, J.; Zhao, Y.; Truhlar, D. G. *J. Phys. Chem. A* **2007**, *111*, 4632.